Solar Physics
DOI: 10.1007/●●●●●-●●●-●●●-●●●●-●

Towards Waveform Heliotomography: Observing Interactions of Helioseismic Waves with a Sunspot

Junwei Zhao · Alexander G. Kosovichev · Stathis Ilonidis

© Springer ●●●●

Abstract We investigate how helioseismic waves that originate from effective point sources interact with a sunspot. These waves are reconstructed from observed stochastic wavefields on the Sun by cross-correlating photospheric Doppler-velocity signals. We select the wave sources at different locations relative to the sunspot, and investigate the p- and f-mode waves separately. The results reveal a complicated picture of waveform perturbations caused by the wave interaction with the sunspot. In particular, it is found that for waves originating from outside of the sunspot, p-mode waves travel across the sunspot with a small amplitude reduction and slightly higher speed, and wave amplitude and phase get mostly restored to the quiet-Sun values after passing the sunspot. The f-mode wave experiences some amplitude reduction passing through the sunspot, and the reduced amplitude is not recovered after that. The wave-propagation speed does not change before encountering the sunspot and inside the sunspot, but the wavefront becomes faster than the reference wave after passing through the sunspot. For waves originating from inside the sunspot umbra, both f- and p-mode waves show significant amplitude reductions and faster speed during all courses of propagation. A comparison of positive and negative time lags of cross-correlation functions shows an apparent asymmetry in the waveform changes for both the f- and p-mode waves. We suggest that the waveform variations of the helioseismic waves interacting with a sunspot found in this article can be used for developing a method of waveform heliotomography, similar to the waveform tomography of the Earth.

Keywords: Sun: helioseismology; Sun: sunspots; Sun: oscillations

1. Introduction

Local helioseismology techniques, including time-distance helioseismology (Duvall *et al.*, 1993), acoustic imaging (Chang *et al.*, 1997), and helioseismic holography (Lindsey and Braun, 1997), have been widely used to study solar acoustic wave travel times or phase shifts, which are then used to invert interior structures and flow fields beneath sunspots (*e.g.* Kosovichev, Duvall, and Scherrer, 2000; Gizon, Duvall, and Larsen, 2000; Zhao, Kosovichev, and Duvall, 2001; Sun *et al.*, 2002; Zhao, Kosovichev, and

W.W.Hansen Experimental Physics Laboratory, Stanford University, Stanford, CA94305-4085, USA email: junwei@sun.stanford.edu

Sekii, 2010). These inversions treated the travel-time shifts as caused by subsurface sound-speed perturbations and plasma flows, and they have provided us the tomographic images of the sunspots' interior properties. However, a picture of how helioseismic waves originating from a point source, including both surface gravity (f-mode) waves and acoustic (p-mode) waves, interact with sunspots has not been systematically studied and visualized observationally. This is complicated because solar waves are excited stochastically (except for rare flare events such as reported by Kosovichev and Zharkova, 1998), and thus the observed wave field represents a superposition of waves excited by many sources randomly distributed in space and time.

To understand the effects of the magnetic field on the propagation of helioseismic waves, theoretical efforts have been made to investigate MHD mode conversions, wave absorptions, and wave interactions with inclined magnetic field lines (Cally, 2005; Cally and Goossens, 2008; Schunker *et al.*, 2008). Numerical simulations have also provided useful approaches to the understanding of how helioseismic waves travel through magnetized areas in more realistic conditions. Recently, Cameron, Gizon, and Duvall (2008) studied how f-mode waves interact with magnetic fields by employing an MHD simulation code (Cameron, Gizon, and Daiffallah, 2007), and then they compared their simulation results with the observed signals in the photosphere by summing cross-correlations along a straight line. A similar approach was taken to study p-mode interactions with a sunspot more recently (Cameron *et al.*, 2010). This has given a successful example of how the solar interior properties can be studied by forward modeling. MHD simulations of helioseismic waves, both f- and p-mode, have also been carried out to study various problems of wave excitation and wave – magnetic-field interactions in 3D models by numerous authors, *e.g.* Khomenko *et al.* (2009), Parchevsky and Kosovichev (2009), Shelyag *et al.* (2009), and Stein *et al.* (2010). Some of these theoretical models and simulations consider waves from a point source. Thus, for comparisons with observations, it is necessary to extract from the observational data the wave propagation and wave – sunspot interaction corresponding to a point source from the observational data.

In this article, we employ a time-distance cross-correlation approach to obtain the wave signals (Green's function) from localized point sources, and give pictures of how the f- and p-mode waves interact with a sunspot. We describe our data and method in Section 2, and present results in Section 3. In Section 4, we present results obtained for negative time lags of the cross-correlation functions ("incoming" waves). Summary and Discussion follow in Section 5.

2. Data and Method

For this analysis, we select a stable, long-lived active region, NOAA AR9787, observed by the Solar and Heliospheric Observatory/*Michelson Doppler Imager* (SOHO/*MDI*; Scherrer *et al.*, 1995) in full-disk resolution Doppler velocities. This same active region was also studied by Cameron, Gizon, and Duvall (2008), Cameron *et al.* (2010), and other works as summarized in Gizon *et al.* (2009). Our analysis period covers from 00:00UT 22 January through 23:59UT 26 January, 2002, a total of five entire days. The shape of the sunspot inside this active region did not significantly change during the observational period. For convenience, the entire data sequence is divided into ten

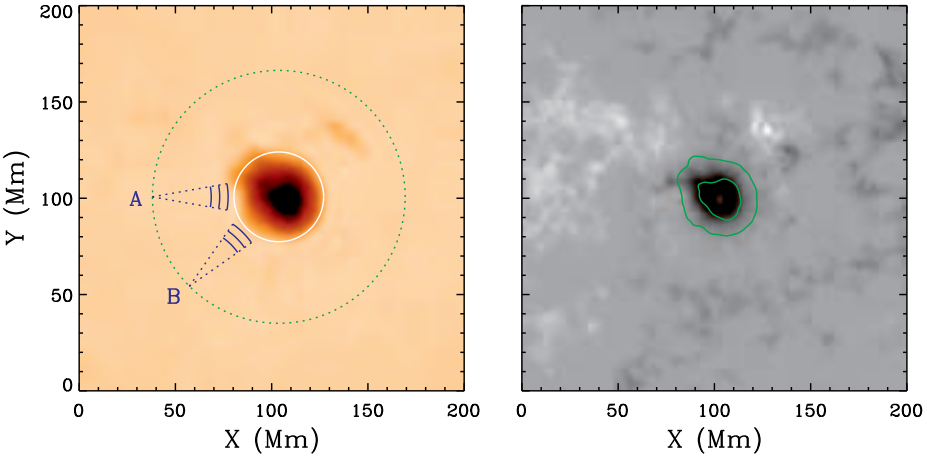

Figure 1. *Left*: Schematic plot over the intensity map of the active region showing how cross-correlation functions are obtained and averaged. Points "A" and "B" are two examples of wave sources, and the green dotted circle shows where wave sources are selected. The white circle indicates that this sunspot is not far from being axisymmetric. *Right*: Magnetogram of this active region, averaged over the entire observation period. The red contours represent boundaries of the sunspot umbra and penumbra.

twelve-hour segments, and each segment is analyzed separately. The cross-correlation functions are obtained from each segment, and then these functions are averaged to get the final waveforms.

As shown in Figure 1, the sunspot located in this active region is not perfectly round but close enough to be considered axisymmetric. Theoretically, if we select location "A" in Figure 1 as a wave source, we can reconstruct the wavefield originating from "A" as a function of time and two-dimensional space by cross-correlating solar oscillation signals at "A" with signals at all other locations inside the area of interest (Claerbout, 1992), using

$$\psi(\tau, \mathbf{d}) = \int f_{\mathrm{A}}(t) f(t+\tau, \mathbf{d}) \mathrm{d}t,$$

where $f_{\mathrm{A}}(t)$ is the observed oscillation signal at location "A", $f(t, \mathbf{d})$ is the oscillation signal observed at a location $\mathbf{d}$ relative to "A", and τ is the time lag between the signals. Zhao *et al.* (2007) have used a similar approach to reconstruct acoustic wave propagation (wavefronts from a point source) in the photosphere and in the interior using the realistic numerical simulations of solar convection (Benson, Stein, and Nordlund, 2006). The cross-correlations provide the wave signals (or Green's function) from an effective point source located at "A". However, to obtain a good signal-to-noise ratio, some averaging over multiple locations is necessary. If we assume that this sunspot is axisymmetric, then we can rotate the wavefield obtained by cross-correlating signals at "B" with all other locations in the area of interst by a certain angle, so that points "A" and "B" coincide, and then we average these two wavefields. Similarly, all locations with the same distance to the sunspot's center, shown as green dotted circle, can be used for averaging. The averaged wavefield provides a Green's function of helioseismic waves propagating from an effective point source to all other areas, including the sunspot. In practice, we do additional averaging. When the wave source is located

outside the sunspot's umbra, we select an area of 3×3 pixels as the center of the dotted green circle, and compute the wavefields for each of these pixels separately. Then we average these wavefields to increase the signal-to-noise ratio.

However, when the wave source is located inside the sunspot umbra, we use all points inside the sunspot umbra for the mean wavefield calculations, and in this case no wavefield rotations are performed before the averaging. It is clear that different number of pixels is used when "A" is located at different distances from the sunspot center, and this would introduce different signal-to-noise ratios in our averaged cross-correlation functions. We compare cross-correlation functions from the sunspot with those from the quiet Sun following the same procedure to reduce this effect, although it is not quite clear how the noise influences our final results.

Our method is similar to the method by Cameron, Gizon, and Duvall (2008) in retrieving wave propagation by calculating cross-correlations. However, we average our signals using a different geometry such that our resultant wave propagation is from an effective point source. This method makes the study of waves' interaction with sunspots simple and straightforward. It also provides observational data that can be easily compared with numerical simulations of waves from point sources. Additionally, the point-source signals effectively represent a Green's function of the wave, which is a primary tool in waveform tomography (Schlottmann, 2009).

3. Results

Because the solar f- and p-mode waves have very different properties, we first separate the f- and p-mode signals in the Fourier domain, and then analyze these two types of waves separately. No other filters, such as a phase-speed filter (Kosovichev, Duvall, and Scherrer, 2000) or a ridge filter (Braun and Birch, 2008), are applied after the mode separation. We use frequencies above 1.8 mHz for the f-mode, and all frequencies above the f-mode ridge for the p-mode analysis.

3.1. Results for p-Mode Waves

For the p-mode waves, we study three different cases: when the wave source is located outside the sunspot, at the boundary of the sunspot penumbra and the quiet Sun, and inside the sunspot umbra.

Figure 2 shows results of the first case, at the 26th, 33rd, and 45th minute of the wave propagation, when the wave source is located 44 Mm from the sunspot center. The selection of this distance is arbitrary, and all pixels at the same distance are used to calculate the cross-correlations. In Figure 2, the left column shows two-dimensional wave propagation images, the middle column shows comparisons of the waveforms of the waves traveling through the sunspot and in the quiet Sun, and the right column shows comparisons of the corresponding oscillations at the given distances. The comparisons with the quiet Sun data in the middle and right columns give a better visualization of differences in the wave propagation and acoustic travel times for the waves with and without interaction with the sunspot. For this case and all following cases, the reference waveforms are obtained for the quiet Sun following exactly the same procedures as for the sunspot study so as to avoid issues such as normalization or different signal-to-noise ratios. At $\tau = 26$ minute, the wavefront enters the sunspot, and the strongest wave

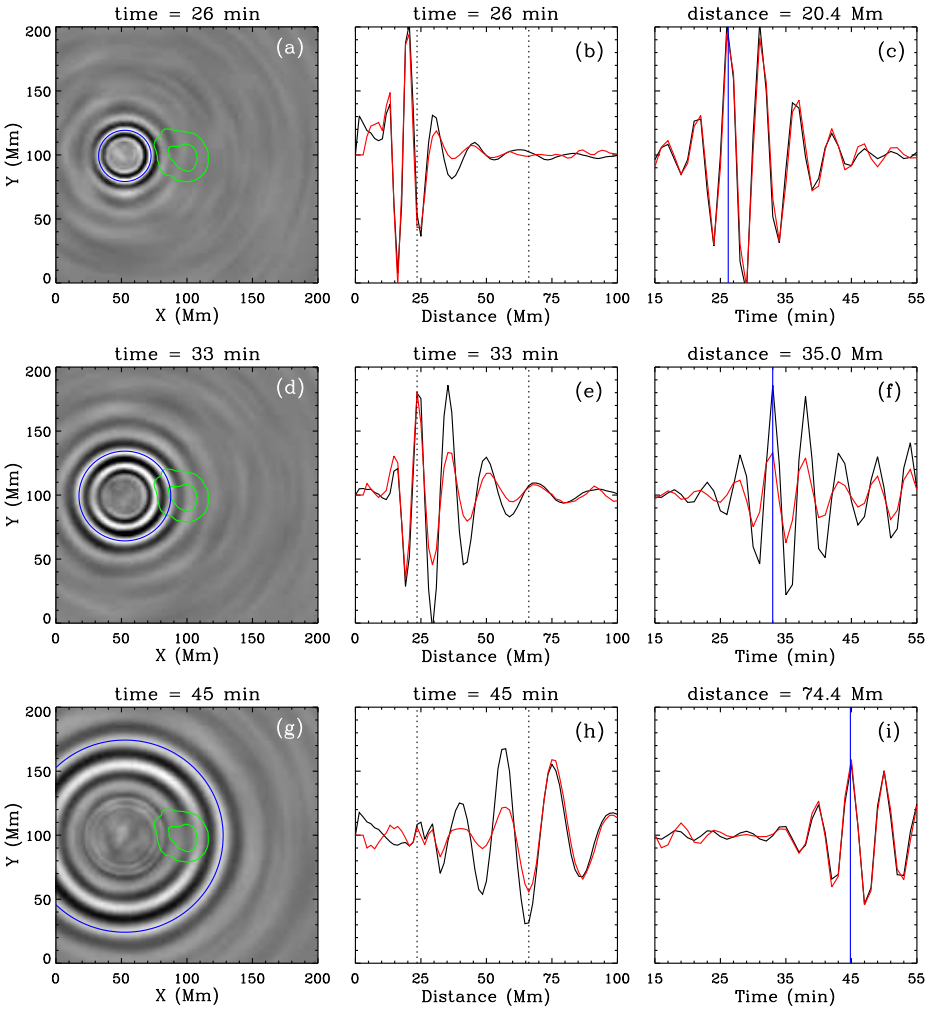

Figure 2. Selected snapshots showing the interaction of *p*-mode waves with the sunspot when the wave source is located outside the sunspot. Left column shows two-dimensional images of the waveform. Red contours indicate the sunspot umbra and penumbra boundaries, and the blue circles show the travel distances obtained for these time moments from the time–distance relation of the quiet Sun. In the middle column, red curves show the waveforms along the line connecting the wave source and the sunspot center, i.e. 0° angle line, in the left images. Black curves are the corresponding waveforms obtained from the quiet Sun, and these are used as reference waves. Vertical dotted lines indicate the two boundaries of the sunspot. In the right column, red curves show oscillations at the location where the blue circles (in the left column) meet the 0° angle line, and dark curves are oscillations from the reference wave at the same propagation distance. The vertical blue lines indicate the reference acoustic phase travel times of the quiet Sun. The travel times are obtained by fitting oscillation functions using Gabor wavelet function. Vertical scales for the middle and right columns are arbitrary.

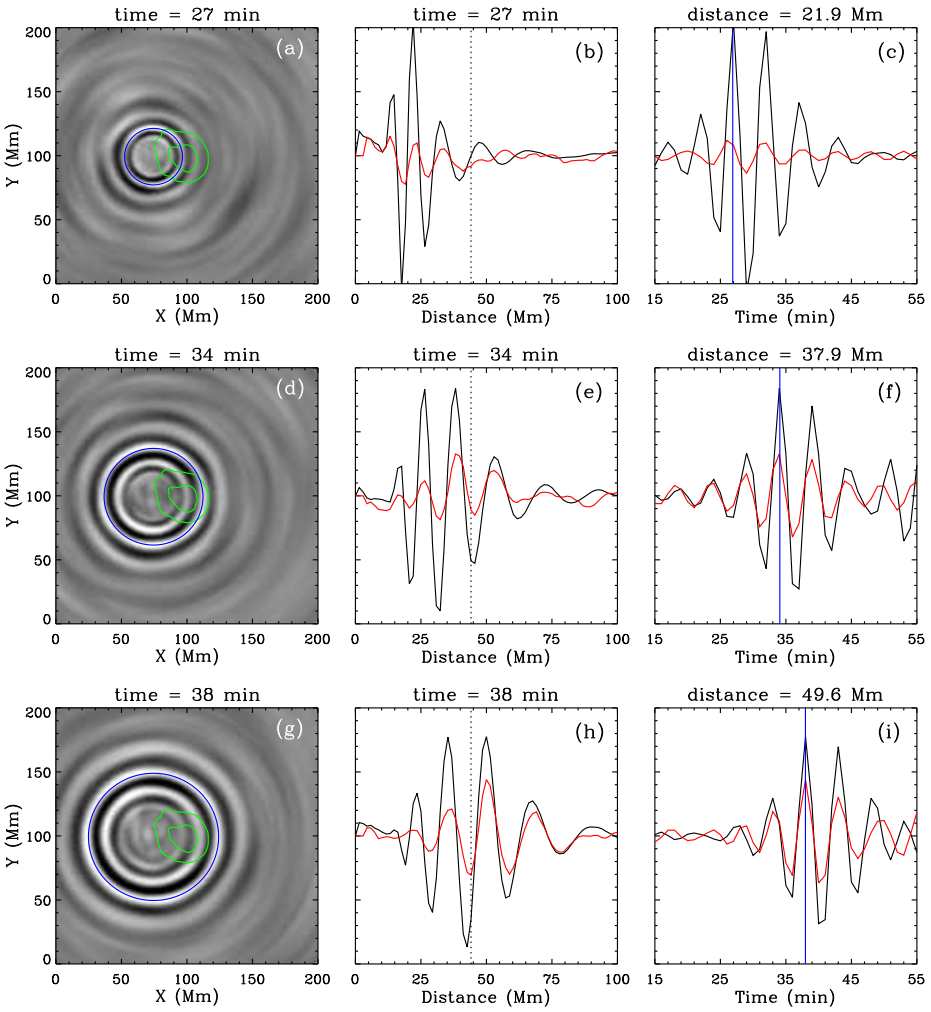

Figure 3. Same as Figure 2, but for a wave source located at the boundary of the sunspot penumbra. The dotted lines in the middle column indicate the penumbra boundary on the opposite side of the wave source.

peak is right outside the boundary of the sunspot. Figure 2(b) shows more clearly that inside the sunspot boundary the wavefront experiences some amplitude reduction and also moves slightly ahead of the reference wave that is obtained from the quiet Sun. The oscillation, shown in Figure 2(c), obtained at the strongest wave peak that is still located outside the sunspot, does not show a noticeable travel-time shift relative to the reference oscillation. At $\tau = 33$ minute, the major wave peak reaches the sunspot umbra, and this wave peak experiences a significant amplitude reduction and moves slightly ahead of the reference wave, as can be seen in Figure 2(e). The oscillations from this wave peak shows that the travel time is approximately 0.3 minutes faster than the reference wave. At $\tau = 45$ minute, the wavefront passes through the sunspot area and arrives at the other side. The comparison of both waveforms and oscillations demonstrates that once the p-mode waves arrive to the other side of the sunspot, the wave does not

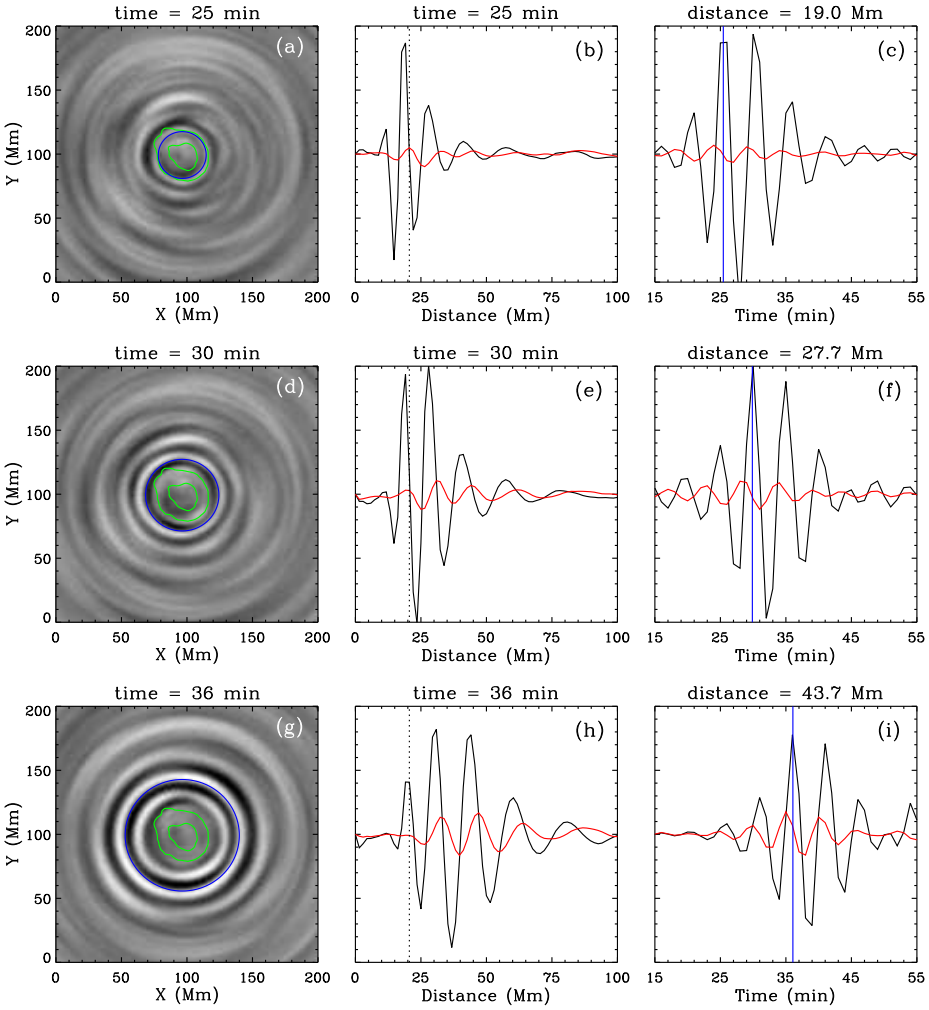

Figure 4. Same as Figure 2, but when the wave sources are located inside the sunspot umbra and averaged over the whole umbra. The dotted line in the middle column indicates the sunspot boundary. Red curves in the middle and right columns are obtained by averaging all propagation directions.

have a noticeable amplitude reduction or travel-time shift. At first sight, it may look strange that the acoustic waves return to their original properties after passing through the sunspot. However, one should keep in mind that the acoustic waves travel through the interior, and that their traveling depths depend on travel distances. The waves that appear on the surface at larger distance travel through the deeper interior, and appear relatively unaffected by the sunspot.

Figure 3 shows the results when the wave source is located at the boundary of the sunspot penumbra and the quiet Sun. At $\tau = 27$ minute, the strongest wave peak reaches the central sunspot area. The comparisons with the reference wave, shown in Figure 3(b) and (c), demonstrate that the wave experiences substantial amplitude reduction, and that this wave peak moves approximately 0.5 minutes ahead of the reference wave. At $\tau =$

34 minute, the major peak is still inside the sunspot and shows faster propagation, while the wavefront outside of the sunspot shows slightly slower propagation. Oscillation sampled right inside the sunspot boundary, shows a slight negative travel time shift of approximately 0.3 minutes. When the large fraction of the wave passes through the sunspot area at $\tau = 38$ minute, shown in Figure 3 (d) – (e), it seems that the wave has roughly the same propagation time as the reference quiet-Sun wave, and experiences some amplitude reduction compared with the reference wave profile. However, this amplitude reduction may be due to the acoustic emissivity reduction at the wave source (Chou *et al.*, 2009; Ilonidis and Zhao, 2010).

Figure 4 shows the results when the wave source is located inside the sunspot umbra. The red curves in the middle and right columns of the figure are obtained by averaging all propagation directions to enhance the signal-to-noise ratio. The reference curves are obtained by the same means. It is clear from the figure that at different propagation time, the wave experiences substantial amplitude reduction, and negative travel-time shifts of approximately 1.0 minute for nearly all locations. This is true for the wavefronts that are still inside the sunspot, and is also true when the wave is very far from the wave source, close to the edge of the analysis area. It is also clear from Figures 4(c), (f), and (i) that the waves originating from the sunspot umbra have roughly the same oscillation period as waves originating from the quiet Sun, i.e. the travel-time shifts are roughly the same for different oscillation peaks.

3.2. Results for f-mode waves

For the f-mode waves, we study two different cases: when the wave source is located outside the sunspot and inside the sunspot umbra.

Figure 5 shows selected snapshots when the wave source is located outside the sunspot, 44 Mm from the sunspot center. Clearly, the f-mode wave propagates much slower than the p-mode waves. It can be found that the wave amplitude reduction starts soon after the wave encounters the sunspot boundary, and the reduction becomes more significant when the wave enters and passes through the sunspot. Unlike the p-mode case, the amplitude reduction does not get recovered after the wave passes the sunspot. For the propagation speed, we find that before the wave encounters the sunspot boundary and during its propagation inside the sunspot (two sample snapshots at $\tau = 37$ and 90 minute are shown in Figure 5), there is no clear difference in the speed or travel times from the quiet-Sun reference. However, when the wavefront passes the sunspot boundary to the outside, at $\tau = 113$ minute, the first peak of the wavefront is clearly ahead of the reference, while the third and fourth peak (counting from the right hand side) are slightly behind the reference wave. This probably indicates a change of the oscillation frequencies and/or the wave dispersion relation inside the magnetized areas. At $\tau = 144$ minute when the wave nearly completely reaches the other side of the sunspot, the first two wave peaks on the right hand side are well ahead of the reference wave. This is similar to the results shown in Figure 4 of Cameron, Gizon, and Duvall (2008).

Figure 6 shows the results when the wave source is located inside the sunspot umbra. The selected snapshots display different propagation times when the entire wave is inside the sunspot boundary, when the wave just leaves the sunspot completely, and when the wave is far from the sunspot. All of these cases show substantial wave amplitude reductions, but this may be due to the suppression of oscillations and reduced

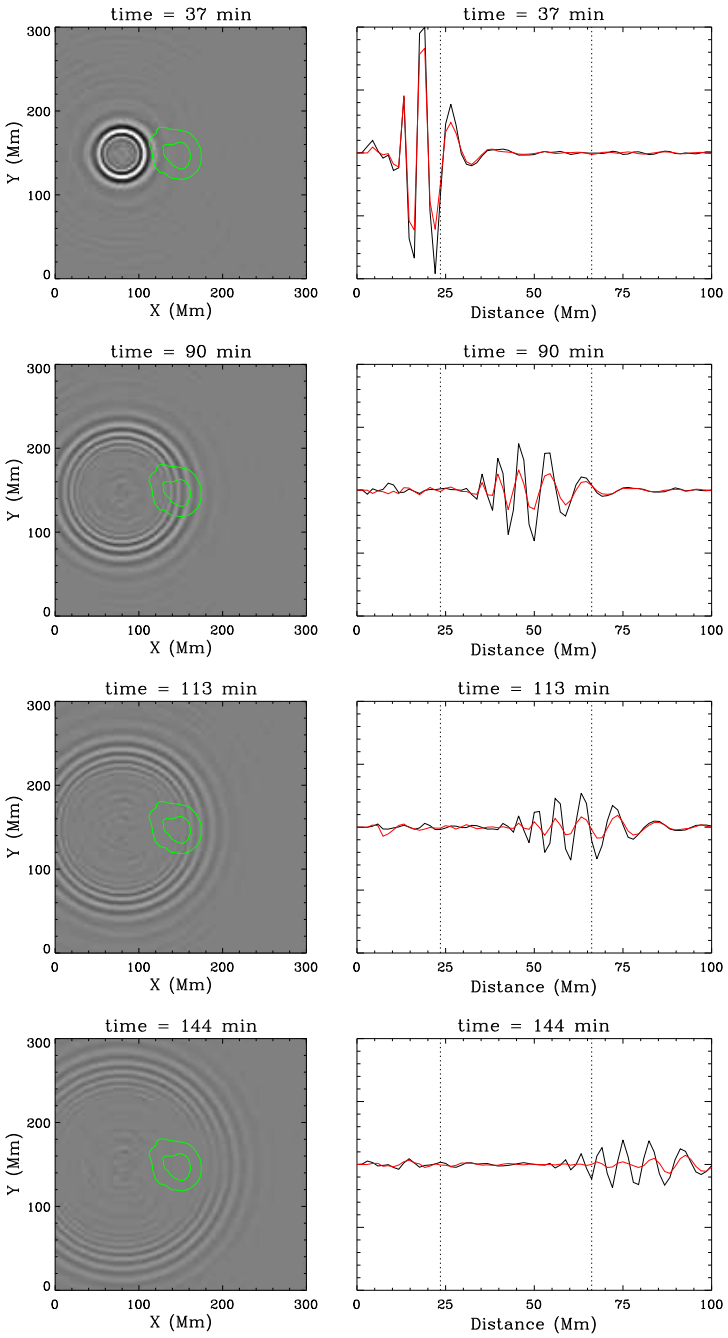

Figure 5. Selected snapshots showing the f-mode wave – sunspot interaction when the wave source is located outside the sunspot. Left column shows two-dimensional images of wave propagation, with red contours indicating the sunspot umbra and penumbra boundaries. In the right column, red curves are horizontal cut through the line linking the wave source and the sunspot center, i.e. 0° angle. Black curves are averaged from the quiet Sun reference wave. Vertical dotted lines represent the sunspot boundaries.

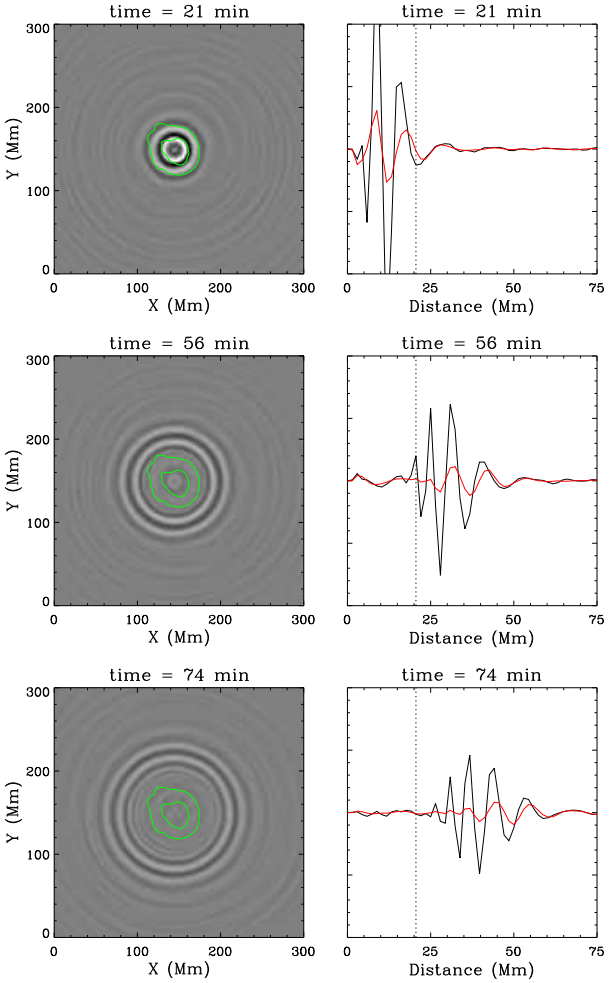

Figure 6. Same as Figure 5, but when the wave source is located inside the sunspot umbra. Dotted lines in the right column represent the sunspot boundary. Red curves are obtained by averaging all wave propagation directions.

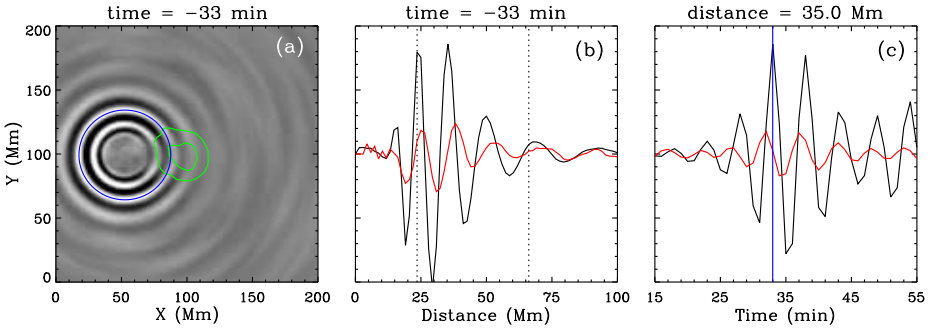

Figure 7. Same as the middle row in Figure 2, but obtained from the negative time lag of the cross-correlation functions.

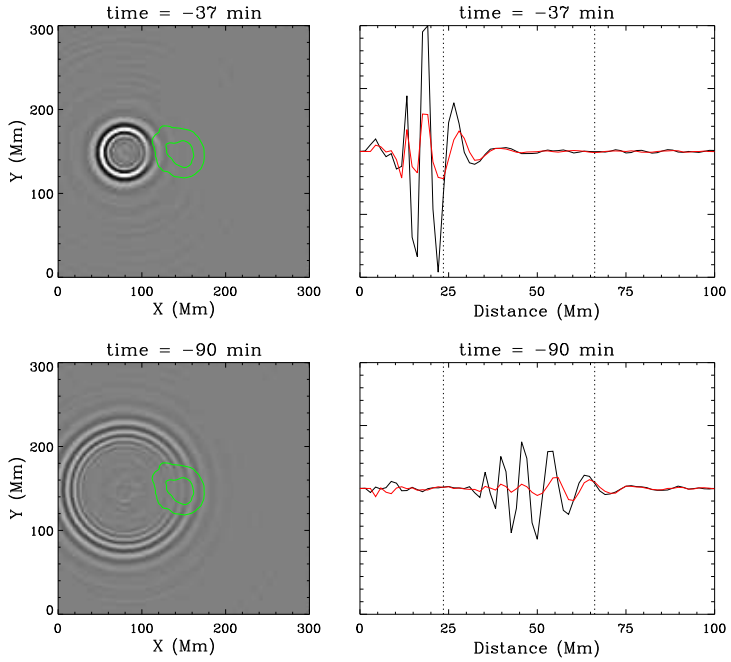

Figure 8. Same as the upper two rows in Figure 5, but obtained from the negative lag of the cross-correlation functions.

wave excitation (Parchevsky and Kosovichev, 2007; Chou *et al.*, 2009). For all of these cases, despite the locations of the wave relative to the sunspot, the first wave peak and sometimes the second wave peak are well ahead of the reference wave, meaning that the f-mode wave originating inside the sunspot umbra always propagates faster than the waves originating in the quiet Sun.

4. Properties of Cross-Correlations with Negative Time Lag

The cross-correlations computed from observed data can have both positive and negative time lags. While the positive time lag of the cross-correlations correspond to waves expanding from the wave source, the negative lag can be understood as waves originating from locations surrounding a selected wave source and converging toward that source. It is interesting to compare the results obtained from these negative time lags with those obtained from the positive lags.

Figure 7 shows one example of p-mode waves when the wave source is located outside the sunspot. Comparing this figure with the results for the expanding waves (positive time lag), shown in Figure 2(d) – (f), one can identify obvious differences between these two sets of results. Figure 7(a) shows that the waveform exhibits an obvious protruding shape inside the sunspot, meaning that the waves starting inside the sunspot and traveling to the outside are significantly faster than the waves starting from the quiet Sun and traveling into the sunspot. Figure 7(b) and (c) more clearly demonstrate this, and the travel-time difference in this case can be as large as 1.0 minute.

Our results for the converging f-mode waves also demonstrate obvious differences from the expanding waves, which can be easily seen by comparing Figure 8 with Figure 5. For instance, at $\tau = -37$ minute, the wave amplitude is significantly reduced even for the waveform outside the sunspot. It shows an obviously faster propagation speed inside the sunspot. At $\tau = -90$ minute, the two peaks on the right hand side show clear shifts. These are not found, or not clear, in the expanding waves. These sharp differences, or asymmetry, between the expanding and converging waves, are very interesting and worth more study. Of course, the converging waves can be reproduced only in numerical simulations with multiple sources.

5. Summary and Discussion

We have analyzed the interactions of helioseismic waves with a round sunspot after separating the p- and f-mode oscillation signals but without using any other signal filters, such as phase-speed filter or ridge filter. By calculating cross-correlation functions from the observed stochastic wavefield, we have reconstructed the wave signals corresponding to effective point sources (Green's function). For both types of waves, we have studied different cases when the wave source is located at different places relative to the sunspot.

We summarize our findings as follows:

- For p-mode waves:
  - *i*) When the wave source is located far outside the sunspot, the wave passes through the sunspot area with a reduced amplitude and slightly shorter travel times. Once the wave reaches the other side of the sunspot, the wave shows little difference from the reference quiet-Sun wave. However, the negative lags (corresponding to converging waves) of cross-correlation functions show a protruding shape inside the sunspot, meaning that waves originating inside the sunspot propagate faster toward the outside.
  - *ii*) When the wave source is located at the boundary of the sunspot, the wave propagates faster inside the sunspot than in the quiet Sun. However, once the wave reaches the other side of the sunspot, the waveform becomes very similar to the reference wave as if the wave does not much effected by the sunspot interior.
  - *iii*) When the wave source is located inside the sunspot umbra, its travel time to areas outside of the sunspot is ≈ 1.0 minute shorter than for the reference waves. The wave amplitude remains substantially reduced at all different locations, but this may due to the reduced acoustic emissivity inside the active region.
- For f-mode waves:
  - *i*) When the wave source is outside the sunspot, the wave amplitude gradually decreases with the propagation through the sunspot. The decreased wave amplitude does not recover after the wave reaches the other side of the sunspot. Before the wave touches the sunspot, and when it propagates inside the sunspot, the propagation speed is about the same as in the quiet Sun. However, when

the wavefront passes the sunspot, the part of the wave outside of the sunspot is ahead of the reference wave, but the part of the wave still inside the sunspot is behind the reference wave. The wavefront remains ahead of the reference after the wave is completely out of the sunspot area. In contrast, the negative lags of cross-correlation functions show faster propagation speed when the wave starts from inside the sunspot.

ii) If the wave source is located inside the sunspot umbra, the f-mode wave stays ahead of the reference wave even when the wave travels very far outside the sunspot, but this is only true for the leading part of the waveform. The trailing part of the waveform is often in accord with the reference wave.

This study presents a clear picture of how helioseismic waves, both f- and p-modes, interact with a sunspot. These results will be useful for comparing MHD simulations of various sunspot models (e.g. Khomenko *et al.*, 2009; Parchevsky and Kosovichev, 2009; Cameron *et al.*, 2010). However, more importantly, these pictures also pose some challenges to our current understanding of the observed travel-time shifts in the sunspot area.

The f-mode results are particularly puzzling. While the faster propagation of the f-mode waves from the sunspot to the outside can be explained by sunspot outflows or moat flows around the sunspot area (Gizon, Duvall, and Larsen, 2000), it is difficult to explain the results when the wave source is located outside of the sunspot. As shown in Figure 5, no slowness of f-mode waves is observed before the wave encounters the sunspot and during the wave's propagation inside the sunspot. The faster propagation is seen only in the leading part of the waveform, and starts only when the wave appears on the other side of the sunspot. This seems to be inconsistent with the effect of symmetrical outflows.

The apparent travel-time asymmetry between the p-mode waves propagating into and out from the sunspot can be clearly seen in Figures 2 and 7, but this asymmetry is not seen when waves are outside of the sunspot area. The travel-time asymmetry inside the sunspot area has been widely studied and discussed. It was interpreted by a combination of subsurface wave-speed perturbations and flow fields (Kosovichev, Duvall, and Scherrer, 2000; Zhao, Kosovichev, and Sekii, 2010), and by a magnetic "shower-glass" effect (Lindsey and Braun, 2005). However, for a quantitative interpretation it requires a careful comparison of the observed waveform variations with results of numerical simulations for various sunspot models. For consistency with the observations such simulations should be performed for randomly distributed sources, taking into account the non-uniform distribution of sources and changes in their spectral characteristics in strong magnetic field regions. This is important because the non-uniform distribution of sources may affect the cross-correlation signals (Rajaguru *et al.*, 2006).

In addition to such a forward modeling approach, our results show perspectives for developing a new local helioseismology technique: waveform heliotomography. This technique is similar to the seismic waveform tomography in geophysics. Instead of inverting travel times, the waveform tomography inverts both the amplitude and phase information of point-source or cross-correlation signals. It has not been used in seismology as much as the travel-time tomography because it is computationally intensive. However, with faster computers this method becomes more achievable. Our results show that the variations of the waveform, in particular the waveform amplitude, are

significantly larger than the variations of the travel times. This means that the wavefront amplitude is probably more sensitive to the sunspot parameters, and, therefore, may provide more information about the sunspot structure and flows. On the other hand, the strong waveform variations may require non-linear inversion techniques (Schlottmann, 2009). We plan to explore the waveform heliotomography approach in future work.

References

Benson, D., Stein, R., Nordlund, Å: 2006, In Uitenbroek, H., Leibacher, J., & Stein R.F. (eds.) ASP Conf. Ser. 354, Solar MHD Theory and Observations: A High Spatial Resolution Perspective (San Francisco, Astron. Soc. Pac.), 92

Braun, D.C., Birch, A.C.: 2008, *Solar Phys.* **251**, 267

Cally, P.S.: 2005, *Mon. Not. Roy. Astron. Soc.* **358**, 353

Cally, P.S., Goossens, M.: 2008, *Solar Phys.* **251**, 251

Cameron, R., Gizon, L., Daiffallah, K.: 2007, *Astron. Nachr.* **328**, 313

Cameron, R., Gizon, L., Duvall, T.L. Jr.: 2008, *Solar Phys.* **251**, 291

Cameron, R.H., Gizon, L., Schunker, H., Pietarila, A.: 2010, *Solar Phys.* this issie. DOI:10.1007/s11207-010-9631-3

Chang, H.-K., Chou, D.-Y., LaBonte, B., TON Team: 1997, *Nature* **389**, 825

Chou, D.-Y., Yang, M.-H., Liang, Z.-C., Sun, M.-T.: 2009, *Astrophys. J.* **690**, L23

Claerbout, J. F.: 1992, *Earth Soundings Analysis: Processing Versus Inversions.* Blackwell Science Inc., New York

Duvall, T.L. Jr., Jefferies, S.M., Harvey, J.W., Pomeranta, M.A.: 1993, *Nature* **362**, 430

Gizon, L., Duvall, T.L., Jr., Larsen, R.M.: 2000, *J. Astrophys. Astron.* **21**, 339

Gizon, L., Schunker, H., Baldner, C.S., Basu, S., Birch, A.C., Bogart, R.S., Braun, D.C., Cameron, R., Duvall, T.L. Jr., Hanasoge, S.M., *et al.*: 2009, *Space Sci. Rev.* **144**, 249

Ilonidis, S., Zhao, J.: 2010, *Solar Phys.* this issue. DOI:10.1007/s11207-010-9611-7

Khomenko, E., Kosovichev, A., Collados, M., Parchevsky, K., Olshevsky, V.: 2009, *Astrophys. J.* **694**, 411

Kosovichev, A.G., Duvall, T.L. Jr., Scherrer, P.H.: 2000, *Solar Phys.* **192**, 159

Kosovichev, A.G., Zharkova, V.V.: 1998, *Nature* **393**, 317

Lindsey, C., Braun, D.C.: 1997, *Astrophys. J.* **485**, 895

Lindsey, C., Braun, D.C.: 2005, *Astrophys. J.* **620**, 1107

Parchevsky, K.V., Kosovichev, A.G.: 2007, *Astrophys. J.* **666**, L53

Parchevsky, K.V., Kosovichev, A.G.: 2009, *Astrophys. J.* **694**, 573

Rajaguru, S.P., Birch, A.C., Duvall, T.L., Jr., Thompson, M.J., Zhao, J.: 2006, *Astrophys. J.* **646**, 543

Scherrer, P.H., Bogart, R.S., Bush, R.I., Hoeksema, J.T., Kosovichev, A.G., Schou, J., Rosenberg, W., Springer, L., Tarbell, T.D., Title, A. *et al.*: 1995, *Solar Phys.* **162**, 129

Schlottmann, R.B.: 2009, arXiv:0905.0239, http://arxiv.org/abs/0905.0239

Schunker, H., Braun, D.C., Lindsey, C., Cally, P.S.: 2008, *Solar Phys.* **251**, 341

Shelyag, S., Zharkov, S., Fedun, V., Erdélyi, R., Thompson, M. J.: 2009, *Astron. Astrophys.* **501**, 735

Stein, R.F., Lagerfjärd, A., Nordlund, Å., Georgobiani, D.: 2010, *Solar Phys.* this issue. DOI:10.1007/s11207-010-9510-y

Sun, M.-T., Chou, D.-Y., Ton Team: 2002, *Solar Phys.* **209**, 5

Zhao, J., Georgobiani, D., Kosovichev, A.G., Benson, D., Stein, R.F., Nordlund, Å.: 2007, *Astrophys. J.* **659**, 848

Zhao, J., Kosovichev, A.G., Duvall, T.L. Jr.: 2001, *Astrophys. J.* **557**, 384

Zhao, J., Kosovichev, A.G., Sekii, T.: 2010, *Astrophys. J.* **708**, 304